Nonlinear Network Dynamics on Earthquake Fault Systems

Paul B. Rundle,[1,*] John B. Rundle,[2,†] Kristy F. Tiampo,[3] Jorge S. Sa Martins,[3] Seth McGinnis,[3] and W. Klein[4]

[1]*Fairview High School, Bolder, Colorado 80309*

[2]*Colorado Center for Chaos & Complexity, CIRES, and Department of Physics, CB 216, University of Colorado, Boulder, Colorado 80309*

[3]*Colorado Center for Chaos & Complexity and CIRES, CB 216, University of Colorado, Boulder, Colorado 80309*

[4]*Department of Physics, Boston University, Boston, Massachusetts 02215 and Center for Nonlinear Science, Los Alamos National Laboratory, Los Alamos, New Mexico 87545*

(Received 6 October 2000; revised manuscript received 16 July 2001; published 14 September 2001)

Earthquake faults occur in interacting networks having emergent space-time modes of behavior not displayed by isolated faults. Using simulations of the major faults in southern California, we find that the physics depends on the elastic interactions among the faults defined by network topology, as well as on the nonlinear physics of stress dissipation arising from friction on the faults. Our results have broad applications to other leaky threshold systems such as integrate-and-fire neural networks.

DOI: 10.1103/PhysRevLett.87.148501 PACS numbers: 91.30.Px, 05.65.+b, 84.35.+i, 91.60.Ba

Understanding the physics of earthquakes is essential if large events are ever to be forecast. Real faults occur in topologically complex networks that exhibit cooperative, emergent space-time behavior that includes precursory quiescence or activation, and clustering of events [1–10]. The purpose of our work reported in this Letter is to investigate the sensitivity of emergent behavior of fault networks to changes in the physics on the scale of single faults or smaller.

To summarize our results, we have found that the statistical distribution of large earthquakes on a model of a topologically complex, strongly correlated real fault network is highly sensitive to the precise nature of the stress dissipation properties of the friction laws associated with individual faults. These emergent, self-organizing space-time modes of behavior are properties of the network as a whole, rather than of the individual fault segments of which the network is comprised.

In order to investigate the effect of changes at small scales on the behavior of the network, we need to construct models of earthquake fault systems that contain the essential physics. General methods for constructing such models have been discussed in Refs. [8,11,12]. Briefly, a network topology is defined in an elastic medium, the stress Green's functions (i.e., the stress transfer coefficients) are computed, frictional properties are defined, and the system is driven via the slip deficit as defined below. The long-range elastic interactions produce mean-field dynamics in the simulations [8]. We focus in this work on the major strike-slip faults in southern California that produce the most frequent and largest magnitude events. To determine the topology and properties of the network, we used the tabulation of fault properties published in Ref. [13]. All major faults in southern California, together with major historic earthquakes, are shown in Fig. 1. Figure 2 shows our model fault network. Each fault was assigned a uniform depth of 20 km, the maximum depth of earthquakes in California, and was subdivided into segments having a horizontal scale of $L \sim 10$ km each.

We now turn to the friction law. Several friction laws are described in the literature [4,14,15]. Here we use a parametrization of recent laboratory experiments [16] in which blocks in surface contact are driven past each other at a constant velocity V. Physically the motion of the blocks can be understood as stick-slip. That is, a region of the sliding blocks becomes stuck until the local shear stress $\sigma(\mathbf{x}, t)$ reaches a failure threshold $\sigma^F(V)$ that is a logarithmic function of V. At this point the block slips an amount $\Delta\sigma/K$ where the stress drop $\Delta\sigma = \sigma(\mathbf{x}, t) - \sigma^R(V)$. Here $\sigma^R(V)$ is residual stress that is also a weak function of V, and K is the stiffness of the material in the block. It is also observed [16] that prior to the discontinuous slip described above, there is a small

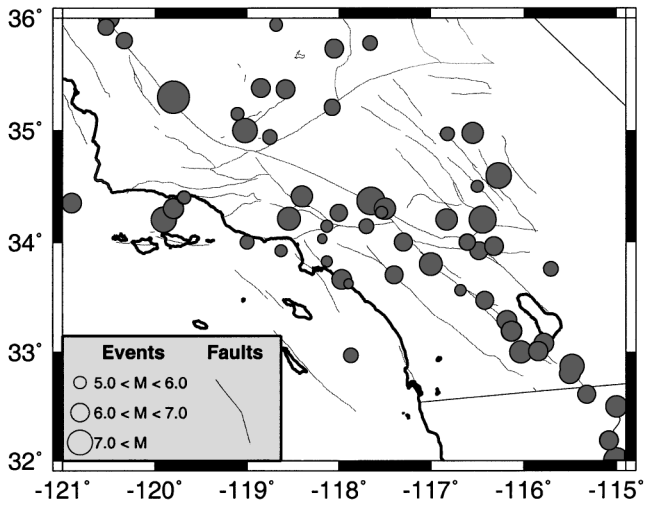

FIG. 1. Map of the major faults in southern California, together with historic earthquakes larger than magnitude 6 (circles) occurring since 1812.

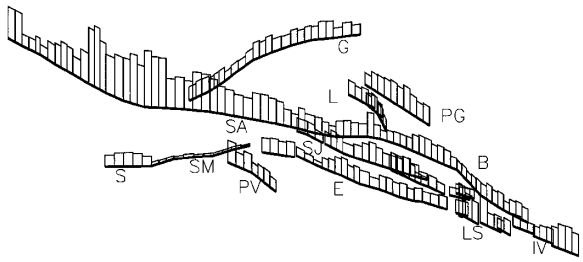

FIG. 2. Major strike-slip faults in southern California used in the model. The difference in frictional coefficients $(\mu_S - \mu_K)$ are shown superposed above each fault, where, if χ_i is the normal stress on fault segment i, then $\sigma_i^F = \mu_{S,i}\chi_i$ and $\sigma_i^R = \mu_{K,i}\chi_i$. The nominal unstable slip on each segment is thus determined by $(\mu_S - \mu_K)$. Fault key: SA, San Andreas; SJ, San Jacinto; E, Elsinore; IV, Imperial Valley; LS, Laguna Salada; G, Garlock; PV, Palos Verdes; S, Santa Cruz Island; PG, Pisgah; B, Brawley; SM, Santa Monica; L, Landers.

amplitude, continuous slip that precedes failure. These observations can be parametrized by the equations [10]

$$\frac{ds(\mathbf{x},t)}{dt} = \frac{\Delta\sigma}{K}\left\{\alpha + \sum_k \delta(t - t_{F,k})\right\} \quad \text{(friction stress)}, \tag{1}$$

$$\sigma(\mathbf{x},t) = K[Vt - s(\mathbf{x},t)] \quad \text{(elastic load stress)}. \tag{2}$$

Here $s(\mathbf{x},t)$ is the slip at $\mathbf{x}$ and t, $s(\mathbf{x},t) - Vt$ is the slip deficit, $\delta(t - t_{F,k})$ is the Dirac delta function, and $t_{F,k}$ is any time t at which $\sigma(\mathbf{x},t_{F,k}) = \sigma^F(V)$. The parameter α, which in this Letter we take as a constant independent of stress, is given by $\alpha = KL/\eta$. Here η is a *surface viscosity* and L is the linear size of a coarse-grained segment over which the stress field $\sigma(\mathbf{x},t)$ is defined. This coarse-grained scale is variable, but it must be smaller than the slip region of the largest earthquakes in the model.

Physically, Eq. (2) states that the stress on a coarse-grained region is the difference between the external loading stress KVt and the stress dissipated by the slip. Equation (1) says that the course-grained slip occurs in two parts: (i) sudden *seismic* slip represented by $\delta(t - t_{F,k})$ and (ii) slow *aseismic* creep occurring on a much longer time scale.

Equation (1) can be obtained from a truncated Taylor series expansion of the coarse-grained, mean-field equation describing a large array of blocks sliding on a frictional surface. Each block is connected to all others via coupling springs, with each block also connected by a load spring to a loader plate translating at velocity V. For that model, it has been shown in Ref. [17] that the equation governing the mean-field dynamics is

$$\frac{\partial\sigma(\mathbf{x},t)}{\partial t} = K_L V - f[\sigma(\mathbf{x},t),V]. \tag{3}$$

Here K_L is the load spring constant, and $f[\sigma(\mathbf{x},t),V]$ is a general functional of $\sigma(\mathbf{x},t)$ and V. Equation (3) is obtained by considering contributions from both the internal energy as well as the entropy, where correct Boltzmann counting applies. If we now model the frictional contact surface in the laboratory sliding experiments of Ref. [16] by the $d = 2$ array of coupled blocks in [17], then we can apply Eq. (3). In the simplest case, the stress $\sigma(\mathbf{x},t)$ is spatially uniform, $\sigma(\mathbf{x},t) \to \sigma(t)$, and then $f[\sigma(\mathbf{x},t),V]$ can be considered as a function, rather than a functional, of $\sigma(t)$ and V. Expanding $f[\sigma,V]$ in a truncated Taylor series in σ around the value σ^R, holding V constant, we find

$$f[\sigma,V] \approx \left.\frac{\partial f}{\partial\sigma}\right|_{\sigma=\sigma^R} \Delta\sigma + \sum_k \Delta f(t - t_{F,k}), \tag{4}$$

where the first term is analytic in σ, and the nonanalytic term $\Delta f(t - t_{F,k})$ parametrizes all the sudden jumps when $\sigma = \sigma^F$. Setting $[\partial f/\partial\sigma|_{\sigma=\sigma^R}] \equiv \alpha/K$ and also $\Delta f(t - t_{F,k}) \equiv [\Delta\sigma/K]\delta(t - t_{F,k})$, and using Eq. (2), we obtain Eq. (1).

The constant α can be seen to play a fundamental role in determining the emergent space-time behavior of a threshold system governed by the kind of *leaky threshold dynamics* described by Eqs. (1) and (2). To illustrate this point simply, we set $\delta(t - t_{F,k}) = 0$ in Eq. (1) and apply Eqs. (1) and (2) to two blocks connected together by a linear spring with spring constant K_C, and to loader plate by a spring with constant K_L. The equations for block 1 are

$$\frac{ds_1}{dt} = \frac{\Delta\sigma_1}{(K_L + K_C)}\,\alpha, \tag{5}$$

$$\sigma_1 = K_L(Vt - s_1) + K_C(s_2 - s_1). \tag{6}$$

An analogous set of equations holds for block 2. If the difference in stress at time $t = 0$ is given by $\delta\sigma(0) = \sigma_2(0) - \sigma_1(0)$, then at a time t later

$$\delta\sigma(t) = \delta\sigma(0)e^{-\beta t}, \quad \text{where } \beta = \alpha\left(\frac{K_L + 2K_C}{K_L + K_C}\right). \tag{7}$$

For $\beta > 0$, differences in stress decay exponentially in time, a process of *stress smoothing*. If $\beta < 0$, a condition that may occur in more general elastic or frictional systems [17,18], variations in stress grow exponentially in time, a process of *stress roughening*. Here we note that $K_C > 0$ corresponds to an *exciting* interaction, while $K_C < 0$ is an *inhibiting* interaction.

Equation (4) is an approximation to $f[\sigma,V]$. Since α is most generally the slope of $f[\sigma,V]$ at constant V, we have $\alpha \to \alpha(\sigma) = K[\partial f/\partial\sigma]$. Therefore α is in general stress dependent and can change on a time scale short compared to the time scale of change for σ^R, σ^F, and K. Since $\alpha \sim \partial f/\partial\sigma$, a given fault in a network can have a positive, a negative, or a zero value of α [17,18], allowing smoothing, roughening, or even smoothing-to-roughening transitions in the case of time-varying stress. Consequently, we will fix all parameters other than α to have values consistent with the behavior of real fault networks and examine the effect of varying α. The details of how to fix the parameters are beyond the scope of this Letter and will be published elsewhere [18].

The model is simulated according to the following rules. Each fault in the network is driven with its own velocity V_i. On each loading time step when failure of a segment does not occur, the segment slides by a small amount proportional to $\alpha_i\{\sigma(\mathbf{x}_i, t) - \sigma^R(V_i)\}$. Note that this type of slip is *stable,* meaning that stress on the segment increases, even though a small amount of sliding occurs. Fault segment i fails via *unstable* slip when its stress reaches the value $\sigma(\mathbf{x}_i, t) = \sigma^F(V_i)$. At failure the fault segment slides so that $\sigma(\mathbf{x}_i, t) = \sigma^R(V_i)$ plus a random overshoot, and part of the released stress is transferred to neighboring segments via the stress Green's function obtained in Ref. [8]. Earthquakes are clusters of segments that have all failed on the same time step. After all sites have a stress below their failure threshold, the faults are loaded again with a velocity V_i.

The results of our simulations are shown in Figs. 3a and 3b in which the Coulomb failure function (CFF), defined as CFF $\equiv \sigma(\mathbf{x}, t) - \sigma^F(V)$, is indicated for the 215 fault segments placed end to end along the horizontal axis. The vertical axis is time. The CFF is represented by the color scheme. High CFF is indicated by the red end of the spectrum and low CFF by the blue end. Large earthquakes are represented by horizontal black lines. A large CFF indicates that the fault segment is nearing failure, i.e., $\sigma(\mathbf{x}, t) \sim \sigma^F(V)$. Figure 3a represents data obtained with

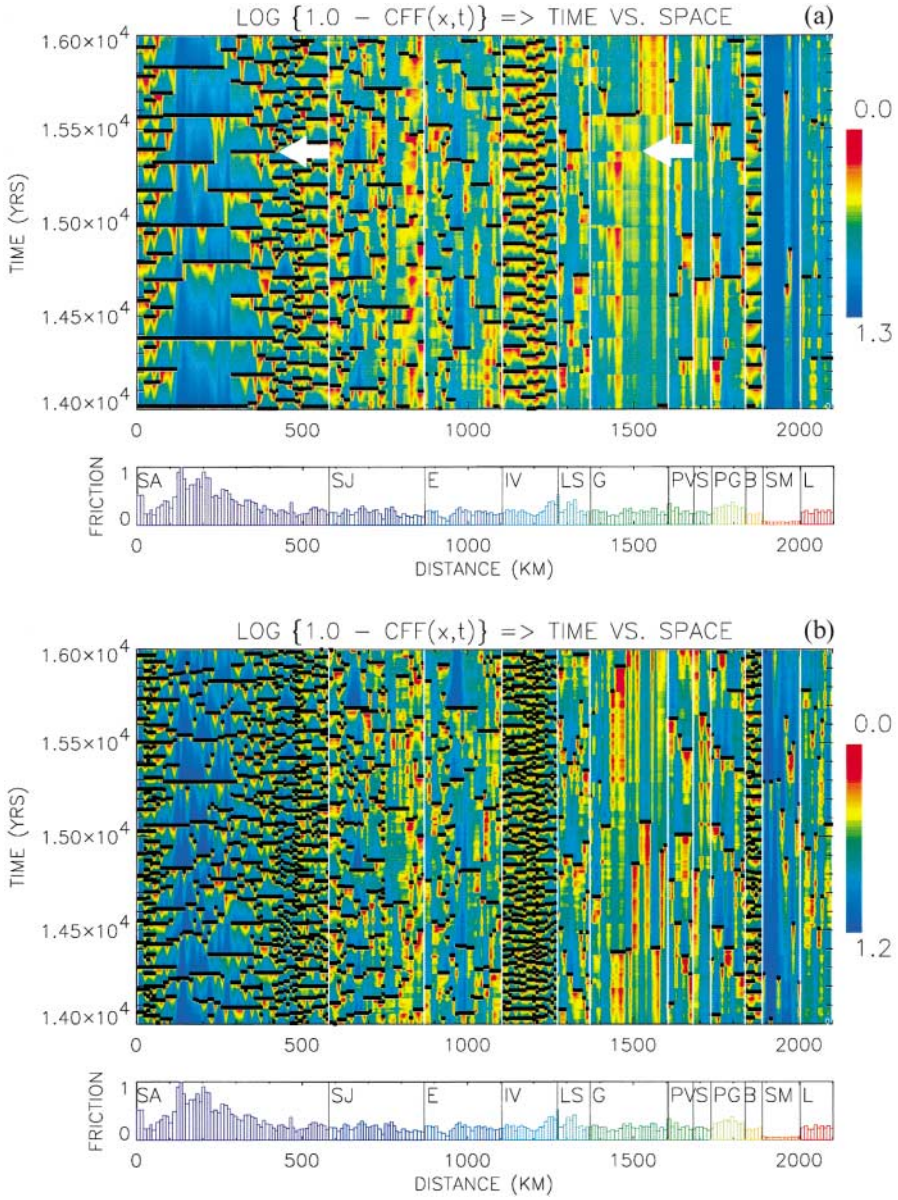

FIG. 3 (color). (a) Plot of Coulomb failure functions plotted as a function of time vs spatial location for 2000 simulation years for a set of values $\{\alpha_i\}$ obtained by approximately matching the ratio of aseismic creep to seismic slip on various fault segments from tabulated data in Ref. [13]. We actually plot Log$\{1 - \text{CFF}(\mathbf{x}, t)\}$, where CFF$(\mathbf{x}, t)$ is in MPa, so that subtle differences can be seen. Low CFF$(\mathbf{x}, t)$'s are represented by cool colors; high CFF$(\mathbf{x}, t)$'s near 0 are represented by hot colors. (b) Same as (a) but with all $\alpha_i = 0$.

nonzero values of α, and in Fig. 3b the value of α is zero. Calculations using the elastic stress Green's functions indicate that both positive (exciting interaction) and negative (inhibiting interaction) stress transfer can occur in a general fault network when a fault segment fails. The nature of the interaction is determined entirely by the network topology and the mathematical structure of the stress Green's functions [11,12].

Comparing Figs. 3a and 3b it is easily seen that the events in Fig. 3a are generally larger than in Fig. 3b. The reason is that nonzero values of α tend to generate more stable slip due to slow stress release that for the most part smooths the stress fields on fault segments. In contrast, $\alpha = 0$ concentrates the stress release in small events that allow the randomness in the dynamics and initial conditions to keep the stress field rough. A roughness length can be defined [10,19] similar to a correlation length. The larger events in Fig. 3a tend to be more periodic (less complexity) and the relatively smaller events in Fig. 3b tend to have a scaling behavior (more complexity).

In addition, large α leads to strong interfault correlations in space and time. An example can be seen in the activity on the Garlock fault which is the sixth fault from the left in Fig. 3a (labeled GAR). The stress Green's function for stress transfer between the Garlock and the San Andreas fault, which is the first segment on the left, produces an inhibiting interaction [10]. Note the increasing redness of the representation of the CFF on the Garlock fault that ends with no large earthquake (horizontal black line). This cutoff or cessation of stress buildup can be associated in each instance with a large event on the San Andreas fault. Large events on the Garlock are generally seen to be associated with an *absence* of a large event on the San Andreas. This type of strongly correlated behavior is not nearly as obvious for $\alpha = 0$ (Fig. 3b).

Our results imply that many of the significant dynamical properties of earthquakes, including the form of the Gutenberg-Richter relation for the fault network, can be understood only in the context of the topologically complex network as a whole, rather than of the individual faults. However, most computational and theoretical work to date has focused on understanding the behavior of single faults, e.g., Refs. [20–22]. There are several other effects of changing α on the fault network which will be reported in a future publication [10]. These results are of a more general interest than their application to earthquake fault networks. They can be extended, for example, to a consideration of models of neural networks [23,24] in which a firing neuron is mapped to a failed fault segment, $\Delta\sigma(\mathbf{x}_k, t)$ is mapped to the current i_k entering the kth neuron, α_k characterizes the current leakiness of the kth neuron, and the elastic interactions are mapped to the synaptic weights between the kth and jth neural connections.

Research by P. B. R. was supported by the Southern California Earthquake Center (Contribution 540) under NSF Grant No. EAR-8920136. Research by J. B. R. was funded by USDOE/OBES Grant No. DE-FG03-95ER14499 (theory) and by NASA Grant No. NAG5-5168 (simulations). K. F. T. and S. M. were funded by NGT5-30025 (NASA), and J. S. S. M. was supported by CIRES/NOAA, University of Colorado at Boulder. W. K. was supported by USDOE/OBES Grants No. DE-FG02-95ER14498 and No. W-7405-ENG-6 at LANL. W. K. acknowledges the hospitality and support of CNLS at LANL. We also acknowledge the generous support by the Maui High Performance Computing Center, Project No. UNIVY-0314-U00.

*Present address: Harvey Mudd College, Claremont, CA 91711.

†Distinguished visiting scientist at Jet Propulsion Laboratory, Pasadena, CA 91125.

[1] Y. Bar-Yam, *Dynamics of Complex Systems* (Addison-Wesley, Reading, MA, 1997).
[2] H. F. Nijhout, L. Nadel, and D. L. Stein, *Pattern Formation in the Physical and Biological Sciences* (Addison-Wesley, Reading, MA, 1997).
[3] R. A. Harris, J. Geophys. Res. **103**, 24 347 (1998).
[4] C. H. Scholz, *The Mechanics of Earthquakes and Faulting* (Cambridge University Press, Cambridge, UK, 1990).
[5] D. D. Bowman, G. Ouillon, C. G. Sammis, A. Sornette, and D. Sornette, J. Geophys. Res. **103**, 24 359 (1998).
[6] J. B. Rundle, W. Klein, D. L. Turcotte, and B. Malamud, Pure Appl. Geophys. (to be published).
[7] S. J. Gross and C. Kisslinger, Bull. Seismol. Soc. Am. **84**, 1571 (1994).
[8] J. B. Rundle, W. Klein, K. F. Tiampo, and S. J. Gross, Phys. Rev. E **61**, 2418 (2000).
[9] R. S. Stein, Nature (London) **402**, 605 (1999).
[10] P. B. Rundle (to be published).
[11] J. B. Rundle, J. Geophys. Res. **93**, 6255 (1988).
[12] S. N. Ward, Bull. Seismol. Soc. Am. **90**, 370 (2000).
[13] J. Deng and L. R. Sykes, J. Geophys. Res. **102**, 9859 (1997).
[14] B. N. J. Persson, *Sliding Friction, Physical Principles and Applications* (Springer-Verlag, Berlin, 1998).
[15] J. Dieterich, J. Geophys. Res. **84**, 2161 (1979).
[16] T. E. Tullis, Proc. Natl. Acad. Sci. U.S.A. **93**, 3803 (1996).
[17] W. Klein, J. B. Rundle, and C. D. Ferguson, Phys. Rev. Lett. **78**, 3793 (1997).
[18] J. B. Rundle, W. Klein, M. Anghel, and J. S. Sa Martins (to be published).
[19] J. B. Rundle, E. Preston, S. McGinnis, and W. Klein, Phys. Rev. Lett. **80**, 5698 (1998).
[20] R. Burridge and L. Knopoff, Bull. Seismol. Soc. Am. **57**, 341 (1967).
[21] J. B. Rundle and D. D. Jackson, Bull. Seismol. Soc. Am. **67**, 1363 (1977).
[22] J. M. Carlson and J. S. Langer, Phys. Rev. A **40**, 6470 (1989).
[23] J. J. Hopfield, Phys. Today **47**, No. 2, 40 (1994).
[24] J. B. Rundle, K. F. Tiampo, W. Klein, and J. S. Sa Martins, Proc. Natl. Acad Sci. (to be published).